

Different metamagnetism between paramagnetic Ce and Yb isomorphs

Atsushi Miyake,^{1,*} Yoshiaki Sato,¹ Masashi Tokunaga,¹ Jumaeda Jatmika,² and Takao Ebihara²

¹*Institute for Solid State Physics, The University of Tokyo, Kashiwa, Chiba 277-8581, Japan*

²*Department of Physics, Shizuoka University, Suruga, Shizuoka, 422-8529, Japan*

(Dated: October 2, 2018)

To solve the puzzle of metamagnetic phenomena in heavy fermion systems, we have compared paramagnetic isostructural Ce and Yb systems, CeNi₂Ge₂ and YbNi₂Ge₂, both of which are located near a magnetic instability. The most intriguing result is discovery of a metamagnetic-like transition in both systems from magnetization measurements in a pulsed magnetic fields. This is the first observation of the metamagnetism for isomorphous Ce and Yb paramagnetic systems. Similar to other metamagnets, the metamagnetic transition fields for both compounds are well scaled by the temperature T_{χ}^{\max} , at which the magnetic susceptibility shows a maximum. In addition, for CeNi₂Ge₂ a peak of nonlinear susceptibility χ_3 appears at approximately $T_{\chi}^{\max}/2$, as for other heavy-fermion metamagnets. In contrast, YbNi₂Ge₂ shows only a sign change for χ_3 at T_{χ}^{\max} , as observed in itinerant metamagnets located near the ferromagnetic critical point. The metamagnetism of CeNi₂Ge₂ corresponds to a typical Kondo lattice system, whereas that of YbNi₂Ge₂ is similar to the nearly ferromagnetic itinerant systems. Other possibilities for the metamagnetic behavior of YbNi₂Ge₂ are also discussed.

I. INTRODUCTION

Metamagnetic phenomena in strongly correlated itinerant electron systems have attracted much attention for a long time. Since the discovery of a nonlinear increase in magnetization M of CeRu₂Si₂ at characteristic fields of $H_m \sim 7.8$ T along the tetragonal c -axis [1], extensive experimental and theoretical studies have been performed. Metamagnetism of CeRu₂Si₂ is regarded as a crossover rather than as a phase transition, and hence referred to as a pseudo-metamagnetic transition. When the system is tuned to the antiferromagnetic (AFM) phase by expanding its volume by chemical pressure, the first-order metamagnetic transition from AFM to the polarized paramagnetic (PPM) phase takes place at H_c [2]. In crossing the critical pressure (p_c) at which the AFM transition temperature T_N suppressed to zero, the metamagnetic transition for CeRu₂Si₂ becomes crossover, e.g. $H_c \sim H_m$ [2, 3]. Another example of metamagnetism is field-induced paramagnetic (PM) to ferromagnetic (FM) transition for the itinerant electron systems located near the FM critical point [4, 5]. When the system is in the PM phase beyond the FM critical endpoint, the metamagnetic transition changes to crossover, as observed in UCoAl [4, 6]. In many itinerant electron systems, such as PM heavy-fermion and nearly FM systems, metamagnetism only appears below T_{χ}^{\max} , where the magnetic susceptibility χ is at a maximum. In addition, H_m is known to be proportional to T_{χ}^{\max} [4, 7]. These facts indicate that metamagnetism and the maximum in χ are dominated by a single energy scale, i.e., they have the same origin.

To reveal the more details of metamagnetism in heavy-fermion systems, we focused on certain aspects of the

well-studied ThCr₂Si₂-type tetragonal Ce and Yb systems as the following aspects. In the tetragonal symmetry, the crystalline electric field (CEF) split the $J = 5/2$ ($7/2$) of Ce³⁺ (Yb³⁺) into three (four) Kramers doublets. When the CEF splitting energy Δ_{CEF} , typically of the order of 100-200 K, is larger than the Kondo temperature T_K , the degeneracy of the doublet ground state must be resolved by forming the magnetic order or heavy-fermion state. The balance between T_K and Δ_{CEF} can be tuned by composition or the external parameters, such as pressure and doping. From the literature [7], only the hexagonal and cubic compounds of the PM Yb-systems were known to show metamagnetism, for example, YbCuAl [8], YbAgCu₄ [9], YbCu₅ [10], and YbT₂Zn₂₀ ($T = \text{Co, Rh and Ir}$) [11, 12]. In this context, the discovery of new examples exhibiting metamagnetism among the PM Yb systems having tetragonal symmetry would be desirable. Given the above issues, we focus on the Ce and Yb isomorphs, CeNi₂Ge₂ and YbNi₂Ge₂. Both compounds crystallize in the tetragonal ThCr₂Si₂-type structure and have PM ground states like CeRu₂Si₂. It is quite rare that both Ce and Yb isomorphs have a PM ground state and therefore this comparison may shed light on the difference or similarity between the $4f$ -electron and hole analogues.

CeNi₂Ge₂ is believed to be located near the AFM instability. At low temperature, the electrical resistivity, specific heat and magnetic susceptibility deviate from the Fermi-liquid description [13, 14]. For example, the low-temperature specific heat divided by temperature exhibits a $-\sqrt{T}$ dependence with large value of the coefficient of electronic specific heat $\gamma = 350\text{--}450$ mJ/mol K² [13–15]. The thermal Grüneisen parameter diverges as $T \rightarrow 0$ [16]. Large γ -value and the diverging of Grüneisen parameter recall to mind CeRu₂Si₂ [17]. Both CeNi₂Ge₂ and CeRu₂Si₂ have the large values exceeding 100 as encountered in many heavy-fermion systems [18, 19]. The temperature dependence of χ for

* miyake@issp.u-tokyo.ac.jp

$H \parallel c$ -axis features a broad maximum at $T_\chi^{\max} \sim 28$ K [20] for CeNi_2Ge_2 , whereas $T_\chi^{\max} \sim 10$ K for CeRu_2Si_2 [1]. The Pd substitutions at the Ni sites of CeNi_2Ge_2 induce AFM ordering, which indicates proximity to an AFM phase. [21–23]. CeNi_2Ge_2 was reported to exhibit metamagnetism at $H_m \sim 42$ T in free powdered samples [20] and ~ 43 T in oriented powdered samples [24]. Because of the relatively high H_m , the details of metamagnetism for CeNi_2Ge_2 are still unclear.

YbNi_2Ge_2 has the relatively large γ -value of 136 mJ/mol K² [25] and has an intermediate Yb valence of ~ 2.8 at low temperature [26]. Interestingly, χ shows a broad maximum at approximately 50 K, for both $H \parallel a$ and c [25]. Magnetic ordering was observed above $p_c = 5$ GPa [27], at which the Yb valence remains non-integer [26]. Although the magnetic structure above p_c is still not known, a FM interaction is indicated from the magnetoresistance [27]. This fact infers that YbNi_2Ge_2 is located near a FM critical point. This is strikingly different from CeNi_2Ge_2 , which is located near an AFM instability. Moreover, their magnetic easy directions are different, as seen in the susceptibility curves (see Fig. 1). From scaling, $H_m \sim T_\chi^{\max}$, the metamagnetic behavior for both CeNi_2Ge_2 and YbNi_2Ge_2 is expected to be captured using a pulsed magnetic field.

In this paper, we compare the metamagnetic behavior of paramagnetic CeNi_2Ge_2 and YbNi_2Ge_2 obtained from magnetization measurements for fields up to 56 T using a pulsed magnet. Both are located near their respective magnetic critical point: AFM for CeNi_2Ge_2 and FM for YbNi_2Ge_2 ; the magnetic anisotropy is also different, i.e., the easy magnetization c -axis for the former and the easy basal plane for the latter. The main observation here is that both compounds feature a pseudo-metamagnetic magnetization anomalies when the field is applied along the easy magnetization axis or plane. In particular, YbNi_2Ge_2 might be the first example of a PM Yb compound with tetragonal symmetry exhibiting a metamagnetic behavior. Differences appear in their temperature evolutions of magnetization and nonlinear magnetic susceptibility.

II. EXPERIMENT

Single crystals of CeNi_2Ge_2 were prepared by the Czochralski method, and those of YbNi_2Ge_2 were grown by the In-flux method [25]. The temperature dependence of magnetization at 0.1 T is measured using a commercial SQUID magnetometer. Pulsed-magnetic fields up to 56 T were applied using a non-destructive magnet with typical durations of ~ 36 ms installed at the International MegaGauss Science Laboratory of Institute for Solid State Physics at the University of Tokyo. Magnetization in a pulsed field was measured by conventional induction method, using coaxial pick-up coils.

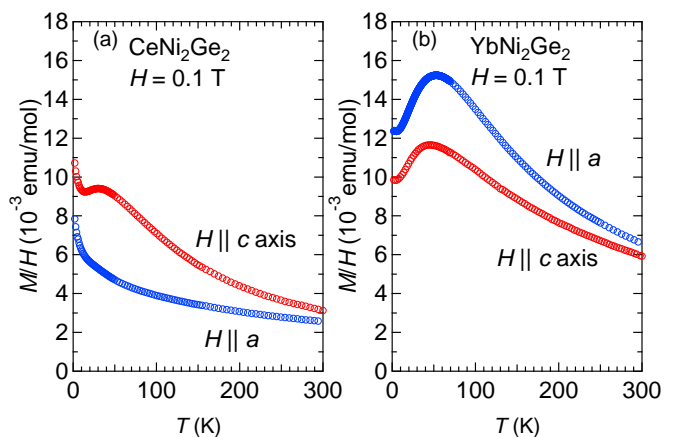


FIG. 1. (color online) Temperature dependence of the magnetic susceptibility M/H of (a) CeNi_2Ge_2 and (b) YbNi_2Ge_2 in magnetic fields of 0.1 T applied along a and c axes.

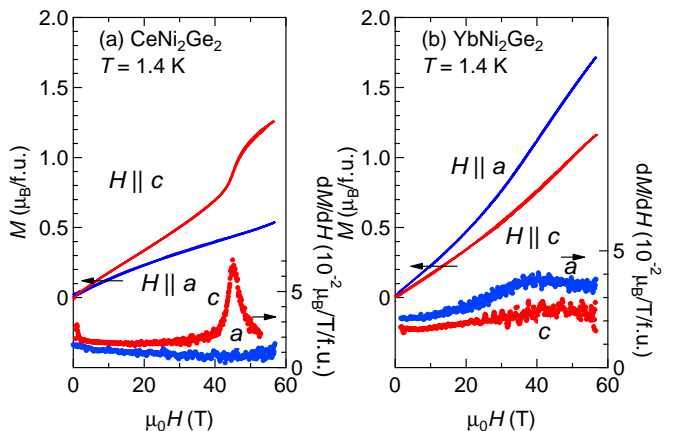


FIG. 2. (color online) Magnetic field dependence of magnetization at 1.4 K of (a) CeNi_2Ge_2 and (b) YbNi_2Ge_2 for $H \parallel a$ and c axes. The differential susceptibility dM/dH for each is also presented.

III. RESULTS AND DISCUSSIONS

Figure 1 presents the temperature dependence of the magnetic susceptibility M/H for applied magnetic fields of 0.1 T along the tetragonal a - and c -axes for CeNi_2Ge_2 and YbNi_2Ge_2 . The overall trends are in good agreement with the previous reports [20, 25, 26]. From the Curie-Weiss fit above 100 K, the effective moment of CeNi_2Ge_2 , estimated to be $\sim 3.0 \mu_B$ for the both directions, is slightly larger than a previous result of $2.84 \mu_B$ [20] and than the expected value of $2.54 \mu_B$ for free Ce^{3+} ion. Although the CEF schemes are still controversial, the splitting energy between the excited and ground states were reported to be 200-300 K [28, 29], which is comparable to the Curie-Weiss fitting temperature range.

To determine effective moment precisely, the susceptibility measurements at higher temperature regions above 300 K are needed. The Weiss temperature $\Theta_{a(c)}$ is evaluated as -206 K (-56 K), which is in agreement with the literature [20]. For YbNi_2Ge_2 , the effective moment is 4.5 (4.6) μ_B , which is near 4.54 μ_B of Yb^{3+} ion, and $\Theta_{a(c)}$ is -79 K (-156 K).

CeNi_2Ge_2 has a maximum in M/H at $T_\chi^{\text{max}} \sim 30$ K for only $H \parallel c$, whereas for YbNi_2Ge_2 a maximum at $T_\chi^{\text{max}} \sim 50$ K appears for both H directions. In addition, the susceptibility of CeNi_2Ge_2 features an upturn at low temperatures. Assuming the anomalous peak corresponds to a density of state of a quasiparticle at the Fermi energy, the increase in χ can be reproduced phenomenologically [14]. The singularity in the density of states relates strongly to the non-Fermi-liquid behavior, which can also reproduce the temperature dependence observed for the specific heat. In addition, the mode-mode coupling theory predicts critical exponents at the AFM quantum critical point giving a $\chi \propto -T^{1/4}$ and a $-T^{1/2}$ dependence for the specific heat. [30]. Although the evaluation of the exponent from Fig. 1 is difficult because low-temperature data are absent, the upturn is a consequence of the proximity to the AFM critical point. The upturn is strongly suppressed with fields, as will be discussed later. In contrast, the susceptibility of YbNi_2Ge_2 monotonically decreases below T_χ^{max} , suggesting that YbNi_2Ge_2 is far from the magnetic instability, in agreement with a previous report [27].

Note also that, by replacing the Ce site by Yb, the magnetic easy direction is switched from the c -axis to the basal plane although the magnetic anisotropy χ_a/χ_c of less than 2 is quite small. Such changes in magnetic anisotropy were also seen for CeRh_2Si_2 and YbRh_2Si_2 [31, 32]. The anisotropy change between CeNi_2Ge_2 and YbNi_2Ge_2 may be due to their different CEFs [25]. With tetragonal symmetry, the magnetic anisotropy is mainly dominated by the $B_2^0 O_2^0$ term of the CEF Hamiltonian, and the easy c -axis and the ab -plane are realized for the negative and positive B_2^0 , respectively [33]. The CEF parameter B_2^0 is evaluated from the difference between Θ_a and Θ_c for $H \parallel a(c)$, specifically, $B_2^0 = 10(\Theta_a - \Theta_c)/[3(2J-1)(2J+3)]$ [25, 34]. Using the estimated $\Theta_{a(c)}$ from the Curie-Weiss fits, B_2^0 for CeNi_2Ge_2 and YbNi_2Ge_2 are respectively estimated as -23 K and 5 K, consistent with their magnetic anisotropy, i.e., the easy c -axis and ab -plane for the former and the latter, respectively.

Our main finding in this work is the discovery of the first example exhibiting metamagnetic-like nonlinear magnetization curves in both isomorphous Ce and Yb compounds having a PM ground state. Figure 2 presents the magnetization curves $M(H)$ at 1.4 K for CeNi_2Ge_2 and YbNi_2Ge_2 for applied fields along a - and c -axes. CeNi_2Ge_2 clearly exhibits metamagnetic behavior at $H_m = 45$ T for $H \parallel c$ -axis, whereas for $H \parallel a$ -axis, M monotonically increases up to the highest fields. This anisotropic behavior, demonstrated here for the first

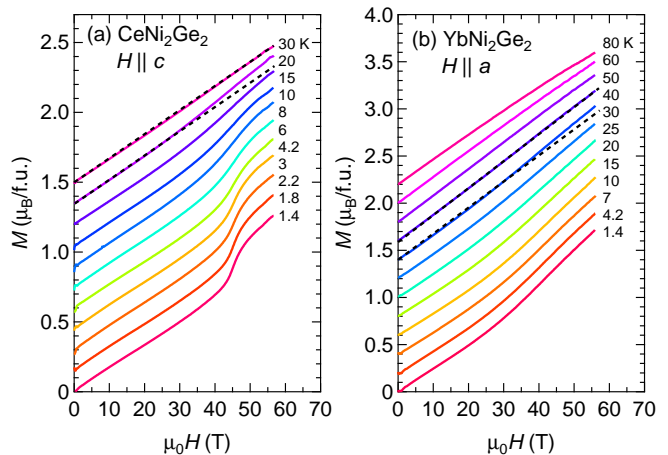


FIG. 3. (color online) Magnetization curves at various temperatures for (a) CeNi_2Ge_2 ($H \parallel c$) and (b) YbNi_2Ge_2 ($H \parallel a$). For clarity, the data are offset by (a) 0.15 and (b) 0.2 $\mu_B/\text{f.u.}$. The dashed lines are extrapolations of the linear field dependence of magnetization, suggesting the disappearance of metamagnetism near T_χ^{max} .

time, is common among Ce PM metamagnets, CeRu_2Si_2 [1] and CeFe_2Ge_2 [35]. Within experimental error, hysteresis is not observed over a field cycle. Moreover, note the $M(H)$ behavior above H_m . In CeNi_2Ge_2 , the linear extrapolation of the $M(H)$ curve above H_m crosses the origin, which is also seen in powdered samples [20]. This is in strong contrast to the isostructural Ce metamagnets, CeRu_2Si_2 [1] and CeFe_2Ge_2 [35]. The finite intercept in CeRu_2Si_2 may reflect the strength of the spin polarization. When crossing H_m , CeNi_2Ge_2 seems to change its PM character to a weakly polarized spin state.

The hole analog YbNi_2Ge_2 exhibits magnetization upturn, which might be the first observation of metamagnetic behavior in a tetragonal Yb paramagnet. Interestingly, the fields along both directions induce magnetization upturns, which may be consistent with the appearance of the peak in the susceptibility at almost identical T_χ^{max} , and therefore the same energy scale governs the maximum of the susceptibility and metamagnetism. The anomaly is clear to see for the easy magnetization a -axis at $H_m \sim 40$ T than that for $H \parallel c$. Contrary to CeNi_2Ge_2 , the nonlinearity of magnetization is very weak as seen in the very broad peak of dM/dH , and M does not tend to saturate at least up to 56 T. The $J = 7/2$ degeneracy is suggested by the susceptibility and the Kadowaki-Woods ratio considering the degeneracy [26, 36]. Higher fields are necessary to saturate to the value 4 μ_B for a free Yb^{3+} ion.

Hereafter, we concentrate on the easy direction, specifically $H \parallel c$ and $H \parallel a$ for CeNi_2Ge_2 and YbNi_2Ge_2 , respectively. Fig. 3 presents the $M(H)$ curves at various temperatures. H_m is insensitive to temperature, and with warming the M anomaly becomes indistinct.

The linearity of $M(H)$ (highlighted by the linear guide lines near T_χ^{\max}) indicates the disappearance of metamagnetism above T_χ^{\max} . In the inset of Fig. 4, the peak of $\chi = dM/dH$ in CeNi_2Ge_2 appears to disappear near T_χ^{\max} . The height of the differential susceptibility of CeNi_2Ge_2 at H_m is determined by $\Delta\chi_m = \chi_m - \chi_0$, where $\chi_{m(0)}$ is the χ at $H = H_m$ (0.1 T). In contrast to the strong temperature dependence of χ_m , χ_0 exhibits very little dependence. $\Delta\chi$ does not diverge at finite temperature, inferring a pseudo-metamagnetic transition. This behavior is also commonly observed in CeRu_2Si_2 and CeFe_2Ge_2 [1, 35, 37].

To extract more details, we replotted M/H as a function of temperature at various constant fields in Fig. 5, with the data from Fig. 3. We first take a look at the characteristics for CeNi_2Ge_2 . With increasing field, the upturn at low temperatures is strongly suppressed and becomes constant at least above 20 T. This indicates the recovery of the Fermi-liquid state. T_χ^{\max} shifts to a lower temperature and tends towards 0 K as $H \rightarrow H_m$. A similar field evolution of the temperature dependence of M/H was also reported for CeRu_2Si_2 [38]. M/H increases further with increasing field and saturates above ~ 50 T. Up to the highest studied fields $H/H_m \sim 1.24$, the suppression of M/H at low temperature seen in CeRu_2Si_2 [38] is not observed. Next, we take a look at YbNi_2Ge_2 . The tendency is similar to CeNi_2Ge_2 , i.e., the broad maximum shifts to lower temperature with increasing field. In contrast to CeNi_2Ge_2 , however, the broad maximum of M/H in YbNi_2Ge_2 does not disappear even above $H_m = 40$ T.

For CeNi_2Ge_2 , T_χ^{\max} is close in energy to the spectral linewidth of the AFM fluctuation obtained from inelastic neutron scattering [15, 39, 40]; unfortunately, a similar measurement for YbNi_2Ge_2 is lacking. Whether the magnetic and/or valence fluctuation exists in YbNi_2Ge_2 is important to know. For CeNi_2Ge_2 , as for CeRu_2Si_2 , the suppression of the AFM fluctuation at H_m drives T_χ^{\max} to zero [41]. Also low-energy spin fluctuations of around 0.6 meV were found to play an important role in the non-Fermi-liquid behavior [40]. Therefore, this low-temperature behavior and the high-field pseudo-metamagnetic transition of CeNi_2Ge_2 are decoupled, as discussed in Ref. [3]. A comparison of the thermal and magnetic Grüneisen parameters may resolve the above issues.

The notable differences between CeNi_2Ge_2 and YbNi_2Ge_2 appear in the temperature dependence of the nonlinear susceptibility χ_3 . The field expansion of the magnetization is written as $M(H) = \chi_1 H + \frac{1}{3!}\chi_3 H^3$, where χ_1 is the uniform magnetic susceptibility and higher order terms are neglected. Therefore, these values can be determined experimentally from the plot of M/H vs H^2 : the intercept and slope correspond to χ_1 and χ_3 , respectively. CeRu_2Si_2 , for example, shows a maximum in both quantities: temperature T_3^{\max} corresponds to a peak in χ_3 that is below T_χ^{\max} [42].

Figure 6 represents the temperature dependence of χ_1

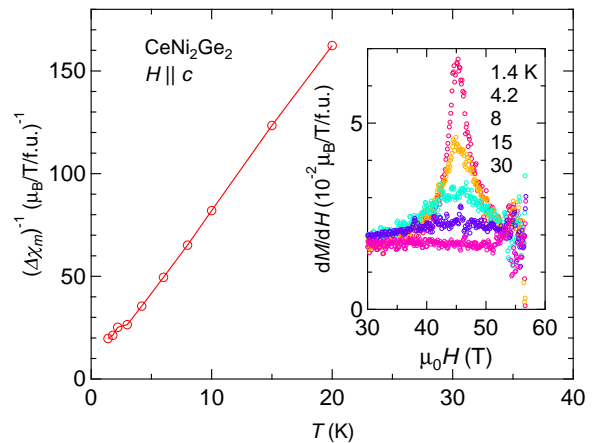


FIG. 4. (color online) Temperature dependence of the inverse peak height of the differential susceptibility of CeNi_2Ge_2 at H_m , $\Delta\chi_m = \chi_m - \chi_0$. The inset shows the temperature evolution of dM/dH .

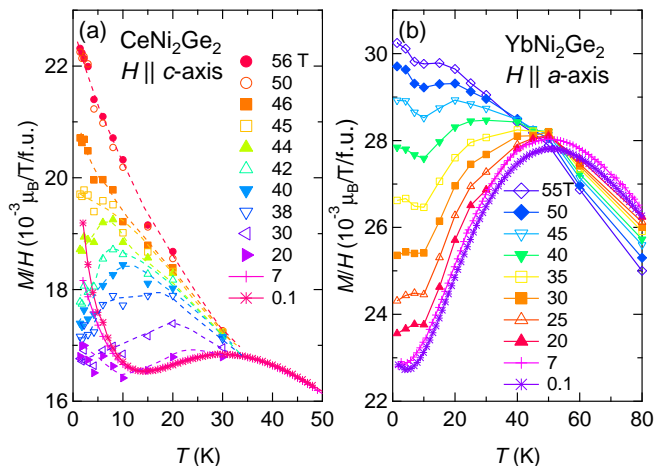


FIG. 5. (color online) Temperature dependence of M/H of (a) CeNi_2Ge_2 ($H||c$) and (b) YbNi_2Ge_2 ($H||a$) at several constant fields. The broken lines in (a) are only a visual guide.

and χ_3 for CeNi_2Ge_2 and YbNi_2Ge_2 , respectively. The consistency between χ_1 obtained from the fit and M/H data measured at $H = 0.1$ T is rather good for YbNi_2Ge_2 . In contrast, the discrepancy is larger for CeNi_2Ge_2 because of the strong field-dependent non-Fermi-liquid behavior in $\chi(T)$ [14]. For CeNi_2Ge_2 , χ_3 exhibits a maximum at $T_3^{\max} \sim 13$ K whereas for YbNi_2Ge_2 χ_3 monotonically decreases with increasing temperature becoming negative at around T_χ^{\max} .

Recently, Shivaram *et al.* pointed out that T_3^{\max} is scaled by T_χ^{\max} in many heavy-fermion systems having a diverse type of metamagnetic transitions [43]. They proposed a simple two-level system model, i.e., an excited pseudospin of $S_z = \pm 1$ separated from the $S_z = 0$ ground

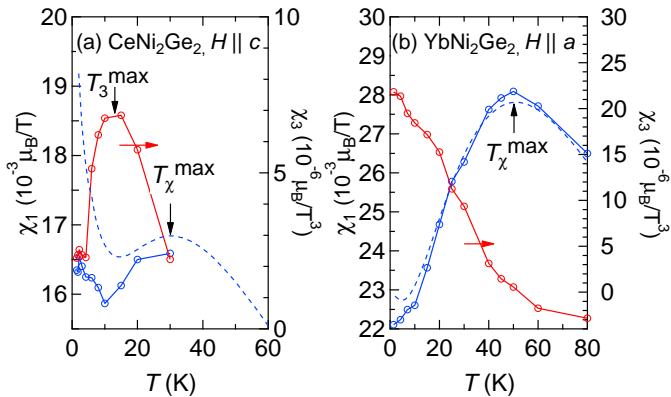


FIG. 6. (color online) Temperature dependence of χ_1 (left axis) and χ_3 (right axis) of (a) CeNi_2Ge_2 for $H||c$ and of (b) YbNi_2Ge_2 for $H||a$, respectively. Symbols and dotted lines are, respectively, fitted results and the M/H measured at $\mu_0 H = 0.1$ T, respectively.

state by a gap Δ yielding the scaling $T_3^{\text{max}}/T_\chi^{\text{max}} \sim 0.4$. The peak structures of χ_1 and χ_3 are dominated by a single energy scale Δ , which is also related to H_m . T_3^{max} of CeNi_2Ge_2 is near $T_\chi^{\text{max}}/2$, following the scaling [43].

In striking contrast, YbNi_2Ge_2 does not show any peak structure in χ_3 . The positive χ_3 gradually decreases with increasing temperature becoming negative at around T_χ^{max} . The universality observed in many heavy-fermion compounds and CeNi_2Ge_2 , i.e., $T_3^{\text{max}}/T_\chi^{\text{max}} \sim 0.4$ [43], is not valid for YbNi_2Ge_2 . The same characteristic behavior, however, were reported in nearly FM itinerant electron metamagnets YCo_2 [44] and TiBe_2 [45], which were not taken into consideration in the literature [43]. The sign change of χ_3 at T_χ^{max} was explained well using Landau theory including the spin fluctuations [5]. The Landau-type expansion uses M as an order parameter, and shown to describe trends for the (nearly) FM systems well. In contrast, for the AFM, the sublattice magnetization needs to be taken into account. Quite recently, the metamagnetism of CeRu_2Si_2 and the related systems were phenomenologically explained using a Landau-type free energy for an AFM Ising systems with two sublattices [46]. The good description for YbNi_2Ge_2 using the usual Landau theory indicates that the metamagnetisms exhibited by CeNi_2Ge_2 and YbNi_2Ge_2 may be different in origin. It was suggested that the FM interaction plays an important role in the magnetically ordered phase of YbNi_2Ge_2 under pressure [27]. And thus, YbNi_2Ge_2 is located near FM critical point at ambient pressure, leading in the similarity to the nearly FM systems. Moreover, most of the pressure-induced magnetic phases of Yb-based systems with ThCr_2Si_2 structure such as YbCu_2Si_2 [47, 48], YbIr_2Si_2 [49] and YbRh_2Si_2 [50, 51] seem to be FM. If the ordered phase above p_c is FM, the field-induced first-order metamagnetic transition from PM to FM is expected near p_c and in the

PM phase [4]. Moving from p_c to the PM side, the transition changes to crossover across the quantum critical endpoint, as found for UCoAl [6]. For YbNi_2Ge_2 , the PM phase is stabilized with decreasing pressure, and thus the metamagnetic crossover may take place at ambient pressure. The broadness of the magnetization anomaly is because the FM critical point is located far away. Pressure experiments can verify this scenario; pressure moves YbNi_2Ge_2 to p_c and changes the metamagnetic anomaly from crossover to first order transition. Of course, an experiment revealing magnetism above p_c is most desired. Because of a lack of other comparisons and experimental investigations of YbNi_2Ge_2 , it is at present difficult to conclude whether metamagnetism has its origin in FM fluctuations.

We discuss other alternative scenarios of the metamagnetic behavior in YbNi_2Ge_2 . The theory based on the Coqblin-Schrieffer model revealed a magnetization upturn for $J = 7/2$ and reproduced the metamagnetic behavior in YbCuAl with a single energy scale; it also explained the maximum in the temperature dependence of magnetic susceptibility and specific heat [8, 52]. In the calculation for $T = 0$, the coefficient of H^2 term of M/H , χ_3 , was found to be positive in agreement with our results [8]. Although there is no theoretical investigation of the temperature dependence of χ_3 , $\chi_3 = 0$ at T_χ^{max} is at least expected with the disappearance of magnetization upturn. A further theoretical investigations of magnetization for $J = 7/2$ at finite temperatures is desired. Metamagnetism in the valence crossover regime is theoretically known [53], in which divergences were seen not only for valence but also magnetic susceptibility at the field-induced valence quantum critical point and thereby initiating FM fluctuations. Indeed, such metamagnetic behavior accompanied by a large valence change is confirmed experimentally in YbAgCu_4 [54]. This may give rise to a similarity between valence changed metamagnets and nearly FM itinerant metamagnets. The very broad $M(H)$ anomaly indicates weak magnetic and valence fluctuations; YbNi_2Ge_2 has a relatively high $p_c \sim 5$ GPa [27]. The evaluation of the field dependences of valence and volume deserves further attention so as to understand the metamagnetic behavior observed in YbNi_2Ge_2 .

Recently, field-induced Lifshitz transitions featuring magnetization anomalies have also been reported, for example in CeRu_2Si_2 [55] and YbRh_2Si_2 [56, 57]. The magnetization anomaly of the latter is a kink rather than a step [58]. For both compounds, the effective mass is reduced across the transition. Notably, the Lifshitz transition is not necessarily accompanied by a magnetization anomaly and a suppression of effective mass, as observed in CeIrIn_5 [59]. For YbNi_2Ge_2 though, excluding the Lifshitz transition as the origin of the magnetization upturn is not possible at present. In this regard, Fermi surface studies across H_m gain some importance and urgency.

Also it is unclear at present whether the metamagnetic behavior of YbNi_2Ge_2 is a specific case or a more general

of PM Yb systems having a tetragonal lattice. Finding other examples such systems exhibiting similar properties and having a susceptibility maximum and easy-plane anisotropy would decide this issue. YbCu_2Si_2 , which is located near the FM phase separated by $p_c \sim 8$ GPa [48], has a susceptibility maximum at $T_\chi^{\text{max}} \sim 40$ K for $H \parallel a$ [60]. At least up to 50 T, however, no clear metamagnetic behavior is observed in YbCu_2Si_2 in any direction, although the anisotropy $\chi_c/\chi_a \sim 3$ and thus CEF are different from that in YbNi_2Ge_2 [60]. Strong differences between CeNi_2Ge_2 and YbNi_2Ge_2 appear in the temperature dependence of M/H near H_m and in χ_3 near T_χ^{max} . To specify the characteristic features in YbNi_2Ge_2 , determining whether other Yb metamagnets such as YbAgCu_4 [9] and $\text{YbT}_2\text{Zn}_{20}$ [12] display a maximum or sign change in χ_3 would be of interest from a substitutional perspective. Although the substitution effect of Ce for Yb are not yet clear, the CEF scheme affects the anisotropy and seems to determine magnetic and/or valence fluctuations. Theoretical investigation considering CEF is strongly desired.

IV. CONCLUSION

From the magnetization measurements in a pulsed field, we have observed the first example of metamagnetic

behavior in PM isomorphs CeNi_2Ge_2 and YbNi_2Ge_2 . The behavior in both is a crossover rather than a phase transition. In contrast to a rather sharp pseudo-metamagnetic transition in CeNi_2Ge_2 , the nonlinearity is very weak for YbNi_2Ge_2 . Similar to other PM systems, the pseudo-metamagnetic fields can be scaled by the temperature corresponding to the susceptibility maximum. Temperature dependence of the linear and nonlinear susceptibility shows strong contrasts between CeNi_2Ge_2 and YbNi_2Ge_2 . The differences seem to depend on whether the systems are located near a AFM or FM critical point. Other possibilities, such as valence fluctuation and Lifshitz transition, are at present not excluded as the origin of the metamagnetic behavior of YbNi_2Ge_2 . These findings are sufficiently intriguing to stimulate further investigations of metamagnetism in these systems.

ACKNOWLEDGMENTS

The authors are grateful to D. Aoki, H. Mitamura, Y. Shimizu, and S. Watanabe for fruitful discussions. This work was partially supported by the MEXT of Japan Grants-in-Aid for Scientific Research (15K17700 and 16H04014).

-
- [1] P. Hean, J. Flouquet, F. Lappierre, P. Lejay, and G. Renenyi, *J. Low Temp. Phys.* **67**, 391 (1987).
 - [2] R. A. Fisher, C. Marcenat, N. E. Philips, P. Haen, F. Lappierre, P. Lejay, J. Flouquet, and J. Voiron, *J. Low Temp. Phys.* **84**, 49 (1991).
 - [3] J. Flouquet, *Progress in Low Temperature Physics* (Elsevier, Amsterdam, 2005), Vol. 15, p. 139.
 - [4] T. Goto, K. Fukamichi, and H. Yamada, *Physica B* **300**, 167 (2001).
 - [5] H. Yamada, *Phys. Rev. B* **47**, 11211 (1993).
 - [6] D. Aoki, T. Combier, V. Taufour, T. D. Matsuda, G. Knebel, H. Kotegawa, and J. Flouquet, *J. Phys. Soc. Jpn.* **80**, 094711 (2011).
 - [7] D. Aoki, W. Knafo, and I. Sheikin, *C. R. Physique* **14**, 53 (2013).
 - [8] A. C. Hewson and J. W. Rasul, *J. Phys. C: Solid State Phys.* **16**, 6799 (1983).
 - [9] T. Graf, J. M. Lawrence, M. F. Hundley, J. D. Thompson, A. Lacerda, E. Haanappel, M. S. Torikachvili, Z. Fisk, and P. C. Canfield, *Phys. Rev. B* **51**, 15053 (1995).
 - [10] N. Tsujii, J. He, F. Amita, K. Yoshimura, K. Kosuge, H. Michor, G. Hilscher and T. Goto, *Phys. Rev. B* **56**, 8103 (1997).
 - [11] S. Yoshiuchi, M. Toda, M. Matsushita, S. Yasui, Y. Hirose, M. Ohya, K. Katayama, F. Honda, K. Sugiyama, M. Hagiwara, K. Kindo, T. Takeuchi, E. Yamamoto, Y. Haga, R. Settai, T. Tanaka, Y. Kubo, and Y. Ōnuki, *J. Phys. Soc. Jpn.* **78**, 123711 (2009).
 - [12] Y. Hirose, M. Toda, S. Yoshiuchi, S. Yasui, K. Sugiyama, F. Honda, M. Hagiwara, K. Kindo, R. Settai, and Y. Ōnuki, *J. Phys.: Conf. Ser.*, **273**, 012003 (2011).
 - [13] P. Gegenwart, F. Kromer, M. Lang, G. Sparn, C. Geibel, and F. Steglich, *Phys. Rev. Lett.* **82**, 1293 (1999).
 - [14] Y. Aoki, J. Urakawa, H. Sugawara, H. Sato, T. Fukuhara, and K. Maezawa, *J. Phys. Soc. Jpn.* **66**, 2993 (1997).
 - [15] G. Knopp, A. Loidl, R. Caspary, U. Gottwick, C.D. Bredl, H. Spille, F. Steglich, and A.P. Murani, *J. Magn. Magn. Mater.* **74**, 341 (1988).
 - [16] R. KÜchler, N. Oeschler, P. Gegenwart, T. Cichorek, K. Neumaier, O. Tegus, C. Geibel, J. A. Mydosh, F. Steglich, L. Zhu, and Q. Si, *Phys. Rev. Lett.* **91**, 066405 (2003).
 - [17] A. Lacerda, A. de Visser, P. Haen, P. Lejay, and J. Flouquet, *Phys. Rev. B* **40**, 8759 (1989).
 - [18] A. de Visser, J. J. M. Franse, J. Flouquet, *Physica B* **161**, 324 (1989).
 - [19] R. KÜchler, P. Gegenwart, C. Geibel, and F. Steglich, *Sci. Technol. Adv. Mater.* **8**, 428 (2007).
 - [20] T. Fukuhara, K. Maezawa, H. Ohkuni, J. Sakurai, H. Sato, H. Azuma, K. Sugiyama, Y. Ōnuki, and K. Kindo, *J. Phys. Soc. Jpn.*, **65**, 1559 (1996).
 - [21] T. Fukuhara, S. Akamaru, T. Kuwai, J. Sakurai, and K. Maezawa, *J. Phys. Soc. Jpn.* **67**, 2084 (1998).
 - [22] G. Knebel, M. Brando, J. Hemberger, M. Nicklas, W. Trinkl, and A. Loidl, *Phys. Rev. B*, **59** 12390 (1999).
 - [23] T. Fukuhara, H. Kadowaki, N. Aso, T. Takeuchi, T. Kuwai, J. Sakurai, and K. Maezawa, *J. Phys. Soc. Jpn.*, **71**, 1360 (2002).
 - [24] P. Gegenwart, J. Custers, T. Tayama, K. Tenya, C. Geibel, G. Sparn, N. Harrison, P. Kersch, D. Eckert,

- and F. Steglich, *Low Temp. Phys.* **133**, 3 (2003).
- [25] S.L. Bud'ko, Z. Islam, T.A. Wiener, I.R. Fisher, A.H. Lacerda, P.C. Canfield, *J. Magn. Magn. Mater.* **205**, 33 (1999).
- [26] H. Yamaoka, I. Jarrige, N. Tsujii, J.-F. Lin, N. Hiraoka, H. Ishii, and K.-D. Tsuei, *Phys. Rev. B* **82**, 035111 (2010).
- [27] G. Knebel, D. Braithwaite, G. Lapertot, P. C. Canfield, and J. Flouquet, *J. Phys.: Condens. Matter* **13**, 10935 (2001).
- [28] T. Kuwai, M. Takeuchi, T. Tsuchiya, Y. Ishikawa, T. Fukuhara, *J. Magn. Magn. Mater.* **272-276** (2004) 68.
- [29] D. Ehm, S. Hüfner, F. Reinert, J. Kroha, P. Wölffe, O. Stockert, C. Geibel, and H. v. Löhneysen, *Phys. Rev. B* **76**, 045117 (2007).
- [30] M. Hatatani, O. Narikiyo, and K. Miyake, *J. Phys. Soc. Jpn.* **67**, 4002 (1998).
- [31] R. Settai, A. Misawa, S. Araki, M. Kosaki, K. Sugiyama, T. Takeuchi, K. Kindo, Y. Haga, E. Yamamoto, and Y. Ōnuki, *J. Phys. Soc. Jpn.* **66** 2260 (1997).
- [32] J. Custers, P. Gegenwart, C. Geibel, F. Steglich, T. Tayama, O. Trovarelli, and N. Harrison, *Acta Phys. Pol. B* **32**, 3221 (2001).
- [33] see for example, P. C. M. Gubbens, *Handbook of Magnetic Materials*, Vol. 20, p. 277.
- [34] Y. L. Wang, *Phys. Lett. A* **35**, 383 (1971).
- [35] H. Sugawara, Y. Aoki, H. Sato, N. Mushnikov, and T. Goto, *J. Phys. Soc. Jpn.* **68**, 1094 (1999).
- [36] N. Tsujii, H. Kontani, and K. Yoshimura, *Phys. Rev. Lett.* **94**, 057201 (2005).
- [37] T. Sakakibara, T. Tayama, K. Matsuhira, H. Mitamura, H. Amitsuka, K. Maezawa, and Y. Ōnuki, *Phys. Rev. B* **51**, 12030(R) (1995).
- [38] K. Ishida, Y. Kawasaki, Y. Kitaoka, K. Asayama, H. Nakamura, and J. Flouquet, *Phys. Rev. B* **57**, 11054(R) (1998).
- [39] B. Fåk, J. Flouquet, G. Lapertot, T. Fukuhara, and H. Kadowaki, *J. Phys.: Condens. Matter* **12**, 5423 (2000).
- [40] H. Kadowaki, B. Fåk, T. Fukuhara, K. Maezawa, K. Nakajima, M. A. Adams, S. Raymond, and J. Flouquet, *Phys. Rev. B* **68**, 140402(R) (2003).
- [41] J. Flouquet, Y. Haga, P. Haen, D. Braithwaite, G. Knebel, S. Raymond, and S. Kambe, *J. Magn. Magn. Mater.* **272-276** 27 (2004).
- [42] J.-G. Park, P. Haen, P. Lejay, and J. Voiron, *J. Phys.: Condens. Matter* **6**, 9383 (1994).
- [43] B. S. Shivaram, D. G. Hinks, M. B. Maple, M. A. de-Andrade, and P. Kumar, *Phys. Rev. B* **89**, 241107(R) (2014).
- [44] D. Bloch, D. M. Edwards, M. Shimizu, and J. Voiron, *J. Phys. F* **5**, 1217 (1975).
- [45] H. Mitamura, M. Takahashi, K. Takizawa, T. Goto, K. Yoshimura, M. Kurasawa, and K. Kosuge, *J. Magn. Soc. Japan*, **23**, 436 (1999).
- [46] K. Matsumoto, S. Kosaka, and S. Murayama, *J. Low Temp. Phys.* **183**, 50 (2016).
- [47] A. Fernandez-Pañella, D. Braithwaite, B. Salce, G. Lapertot, and J. Flouquet, *Phys. Rev. B* **84**, 134416 (2011).
- [48] N. Tateiwa, T. D. Matsuda, Y. Haga, and Z. Fisk, *Phys. Rev. B* **89**, 035127 (2014).
- [49] H. Q. Yuan, M. Nicklas, Z. Hossain, C. Geibel, and F. Steglich, *Phys. Rev. B* **74**, 212403 (2006).
- [50] J. Plessel, M. M. Abd-Elmeguid, J. P. Sanchez, G. Knebel, C. Geibel, O. Trovarelli, and F. Steglich, *Phys. Rev. B* **67**, 180403(R) (2003).
- [51] G. Knebel, R. Boursier, E. Hassinger, G. Lapertot, P. G. Niklowitz, A. Pourret, B. Salce, J. P. Sanchez, I. Sheikin, P. Bonville, H. Harima, and J. Flouquet, *J. Phys. Soc. Jpn.* **75**, 114709 (2006).
- [52] P. Schlottmann, *Phys. Report*, **181**, 1 (1989).
- [53] S. Watanabe, A. Tsuruta, K. Miyake, and J. Flouquet, *Phys. Rev. Lett.* **100**, 236401 (2008).
- [54] Y. H. Matsuda, T. Nakamura, J.-L. HÉR, K. Kindo, S. Michimura, T. Inamai, M. Mizumaki, N. Kawamura, M. Suzuki, B. Chen, H. Ohta, and K. Yoshimura, *J. Phys. Soc. Jpn.* **81**, 015002 (2012).
- [55] M. Boukahil, A. Pourret, G. Knebel, D. Aoki, Y. Ōnuki, and J. Flouquet, *Phys. Rev. B* **90**, 075127 (2014).
- [56] H. Pfau, R. Daou, S. Lausberg, H. R. Naren, M. Brando, S. Friedemann, S. Wirth, T. Westerkamp, U. Stockert, P. Gegenwart, C. Krellner, C. Geibel, G. Zwirnagl, and F. Steglich, *Phys. Rev. Lett.* **110**, 256403 (2013).
- [57] A. Pourret, G. Knebel, T. D. Matsuda, G. Lapertot, and J. Flouquet, *J. Phys. Soc. Jpn.* **82** 053704, (2013).
- [58] P. Gegenwart, Y. Tokiwa, T. Westerkamp, F. Weickert, J. Custers, J. Ferstl, C. Krellner, C. Geibel, P. Kersch, K. -H. Müller, and F. Steglich, *New. J. Phys.* **8**, 171 (2006).
- [59] D. Aoki, G. Seyfarth, A. Pourret, A. Gourgout, A. McCollam, J. A. N. Bruin, Y. Krupko, and I. Sheikin, *Phys. Rev. Lett.* **116**, 037202 (2016).
- [60] N. D. Dung, Y. Ota, K. Sugiyama, T. D. Matsuda, Y. Haga, K. Kindo, M. Hagiwara, T. Takeuchi, R. Settai, and Y. Ōnuki, *J. Phys. Soc. Jpn.* **78**, 024712 (2009).